Texture feature extraction for change detection in drill core images: A comparative study

X. Gu [iD] [a], **N.J. Cook** [a], **A.V. Metcalfe** [b] **and C. Aldrich** [c]

[a] *School of Chemical Engineering, University of Adelaide, South Australia, Australia*
[b] *School of Mathematical Sciences, University of Adelaide, South Australia, Australia*
[c] *Western Australian School of Mines: Minerals, Energy and Chemical Engineering, Curtin University, WA Australia*
Email: xiaomeng.gu@adelaide.edu.au

Abstract: Drill core images provide information of the texture, structure, and mineralogy of the rock, which enables the use of drill core images to optimise downstream processes. The impact on downstream processes from particles of similar composition and mineralogy but different textures has been examined by many researchers. The application of local binary pattern (LBP) and gray-level co-occurrence matrices (GLCM) has been extensively studied by many scholars, and they have been demonstrated to be effective in lithology classification through machine learning techniques. More recently, convolutional neural networks (CNN) with transfer learning for feature extraction have gained attention and have also been proven as an effective tool. Currently, imaging- based data is primarily used in mining for inspection by geologists to support qualitative descriptions. There exists considerable scope for the use of multivariate statistical process control (MSPC) to evaluate imaging data, and an opportunity for the use of image-based data for the detection of subtle changes in rock texture and lithology.

This study builds upon the study of Gu et al. (this volume) and seeks to compare the performance of three widely used feature extraction methods: LBP, GLCM and CNN, for change detection in optical drill core images using MSPC. The results for the GLCM and CNN are consistent with the LBP analysis, and similarly infer that there may exist a major change in lithology mid-way along the length of the drill core. The existence of these two main regimes is also supported by the K-means clustering analysis which is independent of the location of each image. Moreover, the GLCM features are less sensitive to the reference data used to construct the control charts. However, these control charts do show a peak around 160 meters, like the one shown in the control charts for CNN features.

Keywords: *Image analysis, multivariate statistical process control, gray-level co-occurrence matrix, convolutional neural network*

1 INTRODUCTION

Drill core images provide reliable information for mineral exploration and resource characterisation. They provide a visual representation of the geology and mineralization of a mineral deposit or exploration target, and enable geologists to study the texture, structure, and mineralogy of the rocks present. The information obtained from drill core images can be used to determine the quality and quantity of the ore, to estimate the grade and recovery of the mineral, and to design and optimize the mining and processing operations. Moreover, drill core images can help identify the presence of anomalous styles of mineralization, alteration, and other features that are important for exploration and resource estimation. With the development of high-resolution imaging technologies, such as digital photography, hyperspectral imaging, and X-ray computed tomography, drill core images have become increasingly detailed and informative.

Tessier et al. (2007) implemented machine learning techniques to estimate rock mixture composition using rock images for mill feed optimisation, illustrated with a case study of a highly heterogeneous nickel ore system. They demonstrated that the compositions estimated from imaging are in good agreement with the measured values, with correlation coefficients (R^2) of 0.725, 0.903 and 0.844 for soft, medium and hard rock, respectively. Furthermore, correlations between the ore textures and processing response to comminution and/or flotation have been established. Nguyen et al. (2016) predicted parameters of a comminution process using high resolution drill core images. Pérez-Barnuevo et al. (2018) used seven features extracted from grey level co-occurrence matrix (GLCM) and four features from the grey level run-length matrix (GLRLM) as inputs for multivariate discriminant analysis. The results showed significant impact of GLCM statistics for textural classification with accuracy of 88%. The case study conducted on the Mont-Wright iron ore deposit showed a linear relationship between inverse different moment (IDM, statistic for GLCM), short run high grey-level emphasis (SRHGE, statistic for GLRLM) and iron grade, with the model explaining 76% of the variance of the iron grade. Koch et al. (2019) compared 24 combinations of different textural features extraction methods and different classification methods in their case study of the Aitik Cu-Au-Ag deposit, northern Sweden. This, and other studies, have demonstrated the efficacy of using local binary pattern (LBP) and GLCM as feature extraction methods in detecting, classifying, and identifying minerals within specific ore deposits. However, these studies typically require an established drill core texture library as a prerequisite.

In the first part of our study (Gu et al., this volume), a novel machine vision approach was proposed for detecting changes in drill core images using LBP features and multivariate process control, without human intervention. The general strategy is:

- Take photographic images sequentially along the core.
- Summarise each image by a set of features.
- Calculate the principal component analysis (PCA) of the features, based on the correlation matrix, and retain the principal components (PCs) accounting for 80% of the variance of the features. The PCA can be based on either the entire sequence or segments of the sequence, referred to as reference group.
- Calculate Hotelling T^2 and SPE statistics from the PC values for each image, and plot these statistics against image number.

The objective is to compare the performance of LBP with two other feature extraction methods, GLCM and CNN, for change detection, as well as their robustness to noise and artifacts in the images.

2 METHODS

We used the same data as Gu et al. (this volume), which includes the details of the LBP. Brief descriptions of GLCM and CNN follows.

2.1 Gray-level co-occurrence matrix (GLCM)

The GLCM is a widely used method for image texture analysis based on gray-tone spatial dependencies, proposed by Haralick et al. (1973). The image comprises an array of $r \times c$ pixels. The gray tone scale runs from 1 for white up to p for black. If the gray–tone value (gtv) of the pixel at position (x, y), where $1 \leq x \leq r, 1 \leq y \leq c$ is k, we write $I(x, y) = k$, where $1 \leq k \leq p$. A GLCM is a $p \times p$ matrix with entries, (i, j), proportional to the number of instances of pixel pairs in a specified relationship having gtv of i and j. The relationship is defined by the offset, $(\Delta x, \Delta y)$, which indicates that the position of the pairing pixel to the reference pixel is Δx pixels down and Δy pixels to the right. For example, (1,2) indicates one pixel down and two pixels right relative to the reference pixel. The elements of the $p \times p$ GLCM matrix for an offset (Δx, Δy), before normalisation (bn), are:

$$GLCM_{bn(i,j)} = \sum_{x=1}^{r} \sum_{y=1}^{c} \begin{cases} 1, & \text{if } I(x, y) = i \text{ and } I(x + \Delta x, y + \Delta y) = j, \\ 0, & \text{otherwise,} \end{cases} \tag{1}$$

Then each entry in the $GLCM_{bn}$ is normalised to a probability $p(i, j)$, by dividing by the sum of the counts, to give a GLCM matrix P. The calculation of P for a 4×4 image with offset (0,1) is shown in Figure 1.
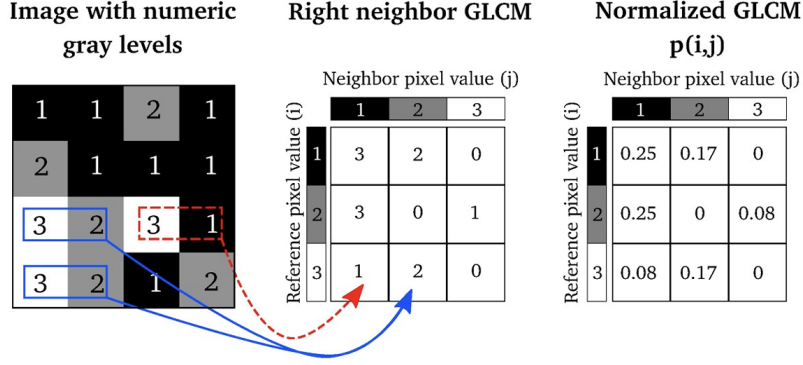

Figure 1. An example of the calculation of GLCM (Löfstedt et al. 2019).

Haralick et al. (1973) proposed 14 statistics of the GLCM as image features, the most often used are contrast, homogeneity, dissimilarity, energy, entropy and correlation. We use these six statistics calculated for each of four offsets, (0,1), (-1,1), (-1,0), and (-1, -1), giving 24 (6 features $\times$ 4 offsets) features for each image.

2.2 Convolutional neural network (CNN)

A CNN is a deep learning model for analysing image data, by learning hierarchical patterns through layers of interconnected convolutional filters. We used VGG16 model (Simonyan & Zisserman 2014), which has been pre-trained on the ImageNet dataset and achieved 92.7% top-5 test accuracy, with architecture shown in Figure 2. The drill core images were resized to a fixed size of 224×224 pixels and CNN works with RGB images. A thousand features are returned from the model, and the first four L-moments (Hosking 1990), mean, L-scale, L-skewness and L-kurtosis, of these features are used for change detection.

Figure 2. The architecture of VGG16 model (Shi et al. 2018).

2.3 Change detection

We have a sequence of 5,982 images, and for each image, LBP, GLCM, and CNN features are calculated, with size of 59, 24, and 4 features, respectively. The PCA using the correlation matrix is implemented to reduce not only the dimension of the features, but also eliminate the correlations between the features, for each feature extraction method. We define the value of PC_j for image i as t_{ij}, and the variance of PC_j is λ_j. Hotelling T^2 is defined as

$$T_i^2 = \sum_{j=1}^{J} \frac{t_{ij}^2}{\lambda_j}, \text{ for } i = 1, \dots, 5982, \tag{2}$$

where J is the number of PCs. Large values of T^2 identify outlying observations. The squared prediction error (SPE) statistic is an alternative indicator of outlying values, and is calculated as follows. We define the features for image i as f_{ik} where k runs from 1 up to M, where M is the number of features for each feature extraction method. We then project these M features onto the first J PCs,

$$SPE_i = \sum_{k=1}^{M} (f_{ik} - \hat{f_{ik}})^2, \text{ for } i = 1, \dots, 5982. \tag{3}$$

Both T_i^2 and SPE_i are plotted against image number, i, as is the custom for MVSPC. To assess the sensitivity of the use of the reference group, a PCA model was fitted to each reference group. The upper 1% quantile of the reference group was used as upper control limit, and is shown as red dashed line in the control charts. The images are divided into five non-overlapping consecutive groups (i.e, in the first group i runs from 1 up to 1,196, in the second group i runs from 1,197 to 2,392 and so on).

3 RESULTS AND DISCUSSION

To provide a contrast to the change detection analysis which takes account of the ordering of the images, particularly when investigating the effects of different reference sets, we performed a K-means cluster analysis which is not influenced by the order of the images. K-means clustering was performed on the GLCM and CNN features, with a chosen K value of 4, to be consistent with the LBP analysis (Gu et al., this volume). The PCA models were implemented to the features of GLCM and CNN, with 4 and 3 PCs obtained, respectively, in order to account for more than 80% variability in the original features.

The application of control charts on GLCM features indicates that they are less sensitive to the choice of reference data when compared to LBP features. Moreover, the cluster analysis does suggest the presence of two regimes that separate along half-way along the drill core (at ca. 350 m). There exists some slight concave pattern for the second half of the drill core when using group 1 and 2 used as reference (Figure 3a – Figure 3d). The absence of substantial differences between the control charts for GLCM features implies a reduced ability to detect changes in texture along the drill core when compared to LBP features. Therefore, we may conclude that LBP features are more effective than GLCM features in identifying changes in textures, at least in the case of this particular dataset. It is noteworthy that the control charts generated consistently identified peaks at approximately 160 meters along the drill core, regardless of the reference data used for PCA model fitting. This observation may imply the presence of significant changes in the textural properties of the rocks at this point.

Table 1. The number of out-of-control images using Hotelling T^2 and SPE control charts with different groups as reference, for each feature extraction method.

	LBP		GLCM		CNN	
	Hotelling T^2	SPE	Hotelling T^2	SPE	Hotelling T^2	SPE
Group 1	2209	280	69	49	17	405
Group 2	1375	1801	795	1471	661	883
Group 3	131	262	174	184	219	224
Group 4	1741	1597	2039	1968	1522	1509
Group 5	292	1177	18	22	119	117

The control charts for the CNN features were initially constructed using CNN features themselves. However, the control charts yield highly inflated values, rendering the results uninformative. Consequently, four L-moments were used to address this issue. The clustering analysis again shows two regimes which are supported by the control charts. Notably, there are peaks at around 160 m for all the control charts, irrespective of which reference data was used. This is consistent with the results returned from GLCM. Moreover, when using group 1 and 2 as reference data, the images in the second half of the drill core stand out (Figure 4a – Figure 4d), whereas they remained relatively stable when other groups are used as reference. When using group 4 as reference, a greater proportion of images from the ~ 200-300 meters segment are detected as outliers, compared with other groups as reference.

Based on the analysis presented in Table 1, the results suggest that the number of outlying images detected by Hotelling T^2 and SPE control charts are relatively consistent across most of the feature extraction methods.

However, significant differences were observed for LBP features when using group 1 and 5 as reference, for GLCM features when using group 2 as reference, and for CNN features when group 1 was used as reference. These differences may be attributed to the variations in the underlying distribution of the feature vectors across different reference groups. Specifically, the reference groups that exhibit higher variability in the feature space may lead to higher detection rates of outlying images, which can be captured by both Hotelling T^2 and SPE control charts.

4   CONCLUSION

Collectively, MSPC control charts work as clustering analysis for detection of changes in terms of segments rather than single images, and our results demonstrate the effectiveness of this approach. Overall, the findings suggest that the application of different feature extraction methods, in combination, can help to reveal distinct patterns and characteristics in the data, even though the methods also show some common patterns. However, the computational complexity should not be neglected; whereas LBP and GLCM provide similar levels of complexity, CNN requires more time to compute even with the pre-trained CNN model. CNN features can be further enhanced by additional training, which will give more detailed textural information, but require higher performance computation. Moreover, the combination of clustering and control charts provides a comprehensive approach for identifying and analyzing potential outliers and changes in the underlying structure of the data. The insights gained from this study can aid in the interpretation of geological data and contribute to the development of effective exploration strategies.

REFERENCES

Gu, X., Metcalfe, A., Cook, N. & Aldrich, C. (2023), *Change detection in drill core images based on local binary pattern [Unpublished manuscript].* Conference Proceedings, MODSIM 2023 (this volume).

Haralick, R. M., Shanmugam, K. & Dinstein, I. H. (1973), 'Textural features for image classification', *IEEE Transactions on systems, man, and cybernetics* (6), 610–621.

Hosking, J. R. (1990), 'L-moments: Analysis and estimation of distributions using linear combinations of order statistics', *Journal of the Royal Statistical Society: series B (methodological)* **52**(1), 105–124.

Koch, P.-H., Lund, C. & Rosenkranz, J. (2019), 'Automated drill core mineralogical characterization method for texture classification and modal mineralogy estimation for geometallurgy', *Minerals Engineering* **136**, 99–109.

Löfstedt, T., Brynolfsson, P., Asklund, T., Nyholm, T. & Garpebring, A. (2019), 'Gray-level invariant haralick texture features', *PloS one* **14**(2), e0212110.

Nguyen, A., Jackson, J., Nguyen, K. & Manlapig, E. (2016), 'A new semi-automated method to rapidly evaluate the processing variability of the orebody', *Proceedings The Third AusIMM International Geometallurgy Conference (GeoMet) 2016, p. 145-152, The Australasian Institute of Mining and Metallurgy: Melbourne.* pp. 145–151.

Pérez-Barnuevo, L., Lévesque, S. & Bazin, C. (2018), 'Drill core texture as geometallurgical indicator for the Mont-Wright iron ore deposit (Quebec, Canada)', *Minerals Engineering* **122**, 130–141.

Shi, B., Hou, R., Mazurowski, M. A., Grimm, L. J., Ren, Y., Marks, J. R., King, L. M., Maley, C. C., Hwang, E. S. & Lo, J. Y. (2018), Learning better deep features for the prediction of occult invasive disease in ductal carcinoma in situ through transfer learning, *in* 'Medical imaging 2018: computer-aided diagnosis', Vol. 10575, SPIE, pp. 620–625.

Simonyan, K. & Zisserman, A. (2014), 'Very deep convolutional networks for large-scale image recognition', *The 3rd International Conference on Learning Representations (ICLR2015)* .

Tessier, J., Duchesne, C. & Bartolacci, G. (2007), 'A machine vision approach to on-line estimation of run-of-mine ore composition on conveyor belts', *Minerals Engineering* **20**(12), 1129–1144.
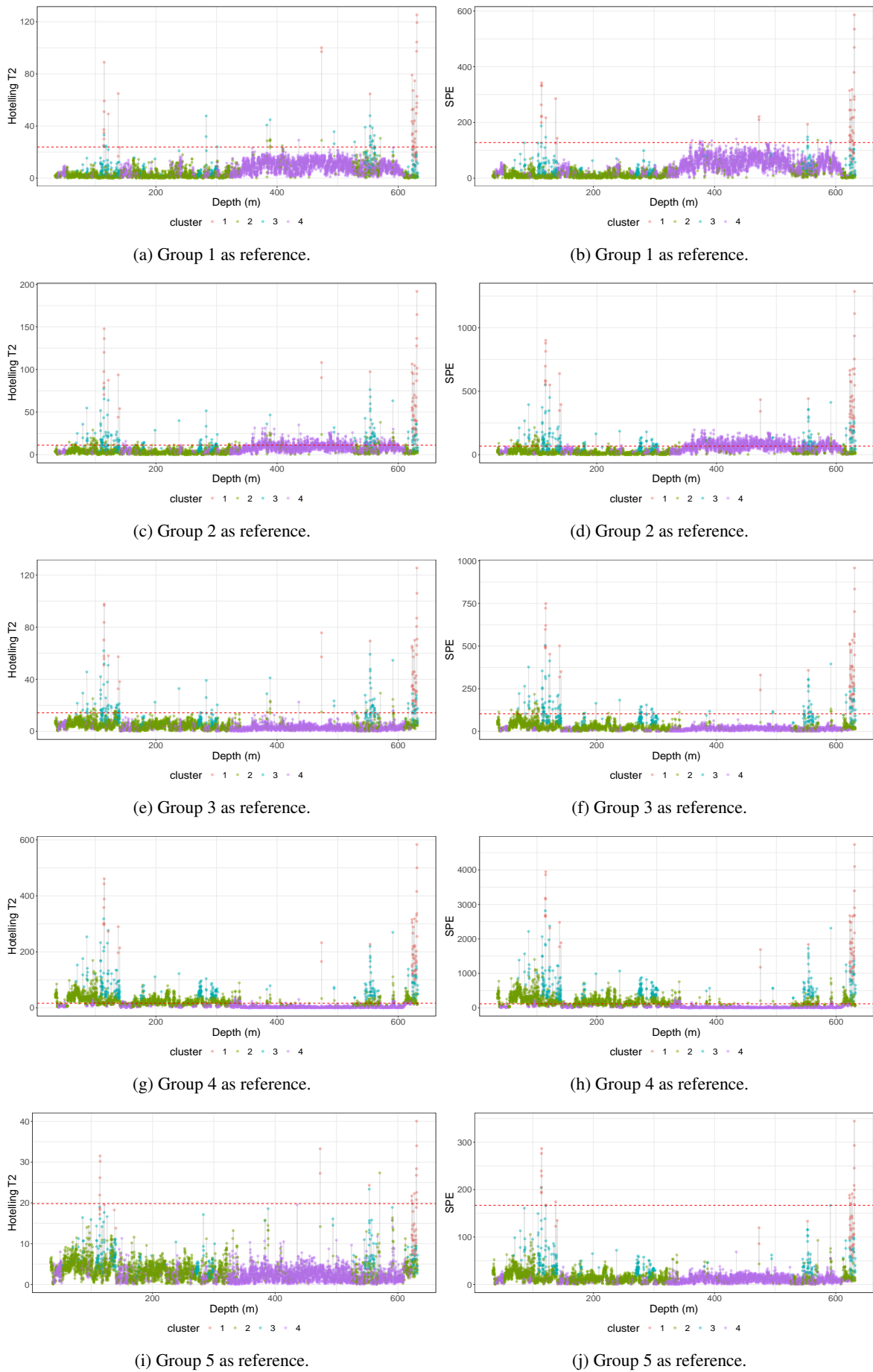
(a) Group 1 as reference.

(b) Group 1 as reference.

(c) Group 2 as reference.

(d) Group 2 as reference.

(e) Group 3 as reference.

(f) Group 3 as reference.

(g) Group 4 as reference.

(h) Group 4 as reference.

(i) Group 5 as reference.

(j) Group 5 as reference.

Figure 3. Hotelling T^2 and SPE statistics calculated using GLCM features, with different groups as reference, colored by 4 different clusters.

(a) Group 1 as reference.

(b) Group 1 as reference.

(c) Group 2 as reference.

(d) Group 2 as reference.

(e) Group 3 as reference.

(f) Group 3 as reference.

(g) Group 4 as reference.

(h) Group 4 as reference.

(i) Group 5 as reference.
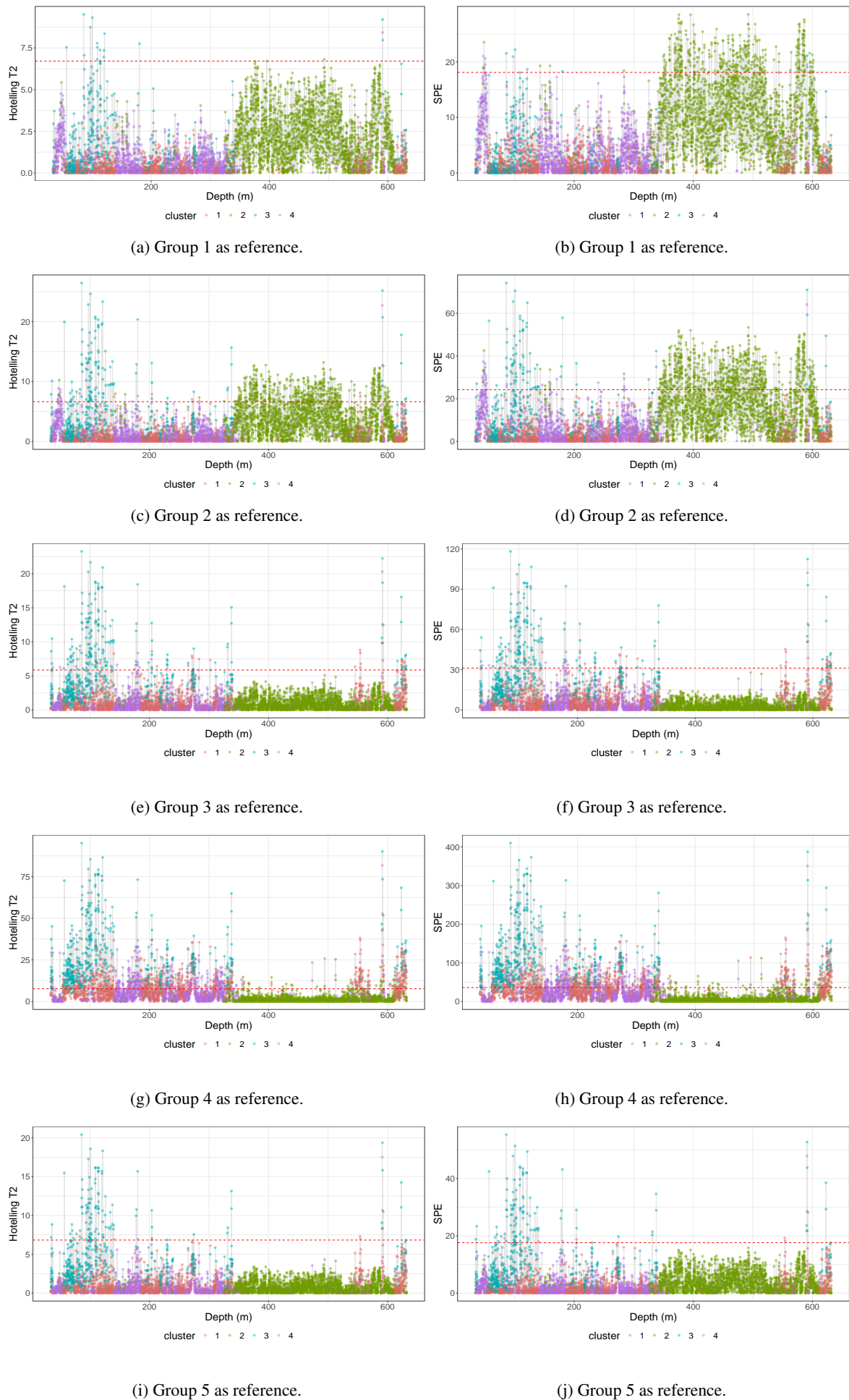
(j) Group 5 as reference.

Figure 4. Hotelling T^2 and SPE statistics calculated using CNN features, with different groups as reference, colored by 4 different clusters.